FINE GRINDING OF FOOD AND FIBROUS MATERIALS

BY

Satoshi Akiyama
Senior Research Scientist
Nisshin Seifun Group Inc.

Carl K. Ishito
General Manager
Nisshin Engineering Inc.

ABSTRACT

A more efficient approach based on numerical simulations for determining optimum blade geometry of the mechanical mill is described. The performance of the mechanical mill with the blades optimized by means of the approach is compared with that of a conventional mechanical mill and a jet mill. In addition, effects of grinding conditions on changes in particle size, color and flavor of the ground materials, which are important properties for food materials, have been investigated.

1. INTRODUCTION

Mechanical impact mills with rotating blades are widely used in the food processing industry for the processing of dry materials because of their efficiency. The demand for fine powder has recently increased in the food processing industry as well as other industries.

In the case of mechanical impact mills, particles are mainly ground by mechanical stresses, including impact and friction. These stresses are caused by the collision of particles with the rotating blades, other particles and stator walls [1]. Therefore, in order to improve the performance of mechanical impact mills, it becomes necessary to understand the flow fields and particle trajectories in such mills because they play an important role in promoting the collision of particles.

Mostly empirical approaches based on experiments are being used for design and optimization of mechanical impact mills. For example, Leschonski and Drogemeier [2] have been carried out experimental studies on the impact speed and the design of an impact machine. However, our understanding of the particle motions in mechanical impact mills is limited.

Recently, computational fluid dynamics (CFD) techniques have been developed and applications of CFD to powder processes have been reported. By use of a three-dimensional numerical simulation technique, Yoshida *et al*. [3] have been carried out a three-dimensional numerical simulation of cyclones. In our previous report [4], the effects of the number of blades and blade angle on the grinding performance of a mechanical impact mill for calcium carbonate particles were studied numerically and experimentally.

In this report, we describe a more efficient approach based on numerical simulations for determining optimum blade geometry of the mechanical mill for fine grinding. The performance of the mechanical mill with the blades optimized by means of the approach is compared with that of a conventional mechanical mill and a jet mill. In addition, we show the effect of grinding conditions on changes in particle size, color and flavor of the ground materials, which are important properties for food materials.

2. EXPERIMENTAL

2.1 Experimental apparatus

Figure 1 shows a schematic diagram of the experimental apparatus used in the studies. Raw materials to be ground were continuously fed into the mill by means of a screw feeder. The raw materials were introduced at the bottom of the mill with surrounding air through the inlet. The materials were then ground by means of swirling shear flow, eddies generated by the blades and impact with the walls. After grinding, the materials were discharged to a bag filter.

Figure 2 shows a cross-sectional diagram of the mechanical impact mill. It is possible to examine a wide range of blade designs by using various fittings on a drive shaft. A cylindrical stator contains a multi-blade rotor, which is driven by a variable-speed motor. The inner wall of the stator has many small grooves. Figure 2 also shows a summary of its geometric dimensions and the definition of the blade angle θ_B. When the blades inclined at a positive value, the inside air is discharged in a downward direction. The number of blades N_B and blade angle θ_B were variables.

Raw materials used for the grinding experiments were wheat bran, dried carrots and green tea leaves. The airflow rate, Q_a, through the mill was measured using an orifice meter and was maintained at 1.5 m^3/min. The powder feed rate, Q_p, was also constant at 1 kg/h.

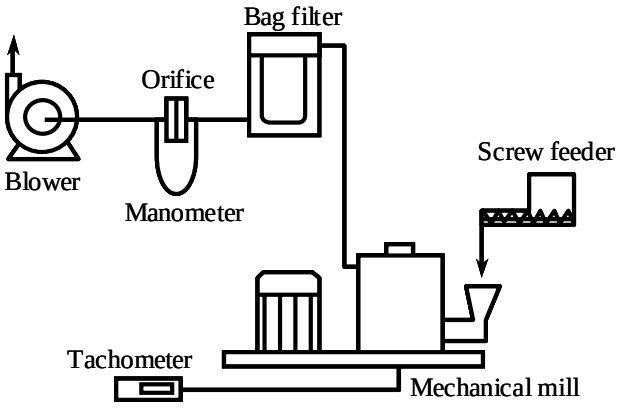

Figure 1 Experimental apparatus

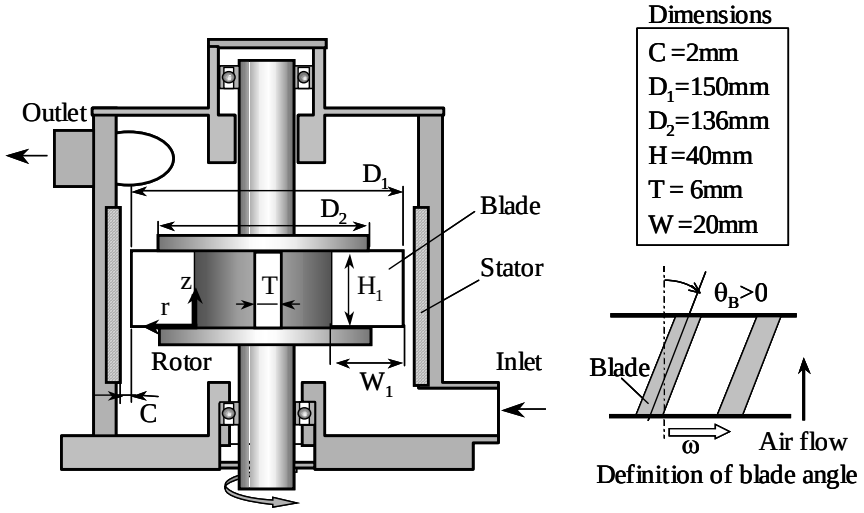

Figure 2 Cross-sectional diagram of mechanical impact mill

2.2 Characterization

Particle size distributions of ground powder were measured by means of a Microtrac particle-size analyzer FSA (Nikkiso, Japan). A tristimulus colorimeter CR-310 (Minolta, Japan) was used to measure color of green tea powder in the CIE L^* a^* b^* color space, defined by CIE (Commission Internationale de I'Eclairage) in 1976. A GC-MS system GC-17A&QP-5000 (Shimazu, Japan) was used to determine flavor of green tea powder ground in the mill.

3. NUMERICAL SIMULATION

3.1 Flow field and particle trajectory

A numerical simulation was conducted to examine how geometry of blades affects particle behavior in the mill. The CFD software Fluent (Ver. 5.5) was used to calculate the flow fields and particle trajectories. Figure 3 shows the calculation region and boundary conditions. The domain enclosed by the two blades, the stator wall and the rotor disks above and below the blades was calculated. The stator was treated as a fixed wall and the rotor was treated as a moving wall. In the simulations, the small grooves on the inner surface of the stator wall were not taken into consideration.

When the Fluent software is used, many models are available for describing turbulent fluid flow. Examples include the standard k-ε model, the renormalization group (RNG) k-ε model, the realizable k-ε model and the Reynolds stress model (RSM). The realizable k-ε model [5], modified for swirling flows, was used in the calculations because of its stability and reasonable

accuracy. The particle trajectories were calculated using a Lagrangian dispersed phase model. Collisions between particles and each wall were assumed to be perfectly elastic, with a coefficient of restitution equal to 1. It was also assumed that particle-particle interactions and the effects of the particle volume fraction on the properties of the surrounding air were negligible. The 100 mono-sized particles were uniformly released at the inlet with a velocity of 0 m/s. The particle density in the calculations was assumed to be the same as the wheat bran (ρ_p = 1,400 kg/m^3) in the experiments.

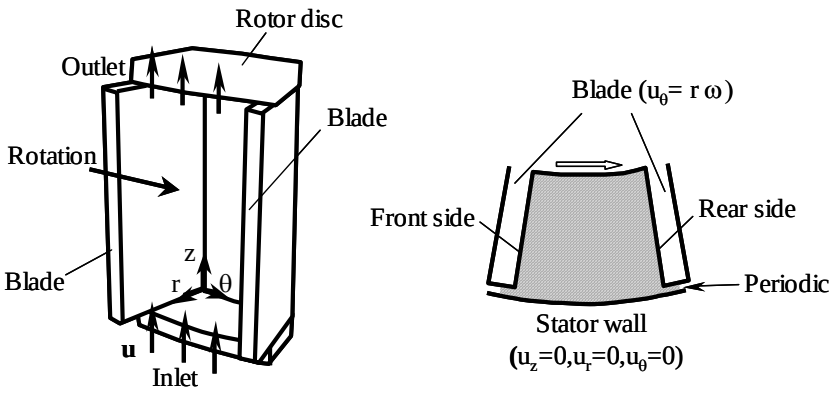

Figure 3 Calculation region

3.2 Impact energy

Using the particle trajectory calculations in the mill, information concerning the residence time of the particles, the number of impacts between the particles and the walls, and the impact velocity were obtained. Finally the energy applied to the particles thorough the grinding zone was estimated.

The impact energy per unit mass for an *i*-th particle for a *j*-th impact are given by:

$$e_{n_{i,j}} = \frac{1}{2} v_{n_{i,j}}^{2} \tag{1}$$

where $v_{n\,i,j}$ is the normal components of the relative velocity of an *i*-th particle.

The total impact energy per unit mass, E_n, is defined as the amount of impact energy applied to a particle in the calculations and the definition is shown as [6]:

$$E_n = \frac{1}{N_t} \sum_{i=1}^{N_t} \sum_{j=1}^{n_i} e_{n_{i,j}} \tag{2}$$

where N_t is number of particles used in the calculations and n_i is total number of impacts for the *i*-th particle.

4. RESULTS AND DISCUSSIONS

4.1 Effect of number of blades

4.1.1 Experimental results

Figure 4 shows the mass median particle diameter, D_{p50}, of wheat bran powder ground under the rotational speed ω = 14,000min^{-1} and the blade angle θ_B = 0^o as a function of number of blades N_B. The median particle diameter of ground powder decreases up to N_B = 16 and then increases.

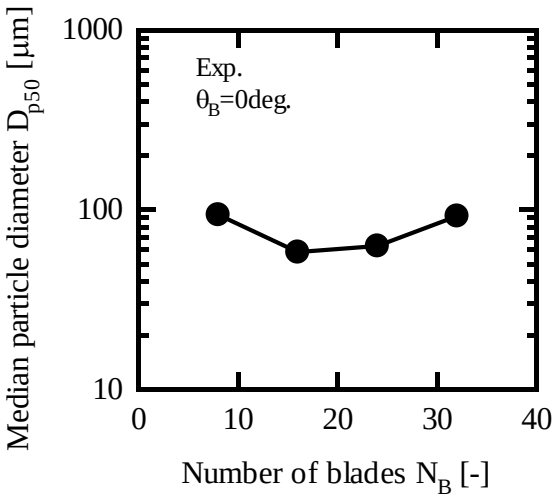

Figure 4 Relationship between median particle diameter and number of blades

4.1.2 Comparison with calculated results

Figure 5 shows the calculated result of the flow field in the mill under the rotational speed ω = 14,000 min^{-1}, the number of blades N_B = 16 and the blade angle θ_B = 0^o. Radial and tangential velocity vectors are indicated in the figure. A strong swirling flow is observed in the mill. Contours of constant pressure on the blade surfaces are also plotted. Pressure is highest near the lower corner of the blade on the front side.

Figure 6 shows the radial and tangential fluid velocity vectors in the r-θ plane at a height of 20 mm for the number of blades N_B = 8, 16 and 32. For N_B = 8, there are a large swirling flow near the blade of the front side and a secondary flow near that of the rear side. For N_B = 16, a large swirling flow between blades appears. Increasing the number of blades N_B to 32, two small vortices near the root of blades are induced by a swirling flow near the tips of blades.

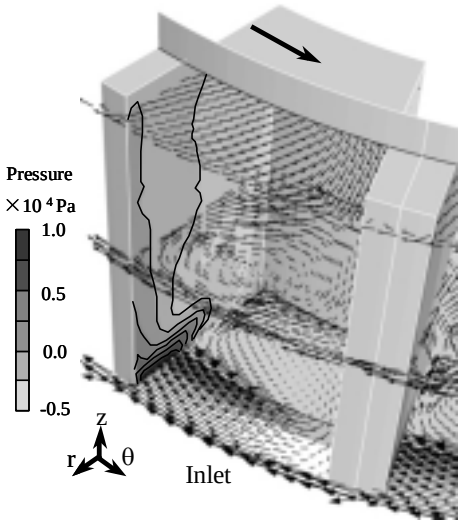

Figure 5 Calculated Velocity vectors and pressure contours for N_B=16, θ_B=0

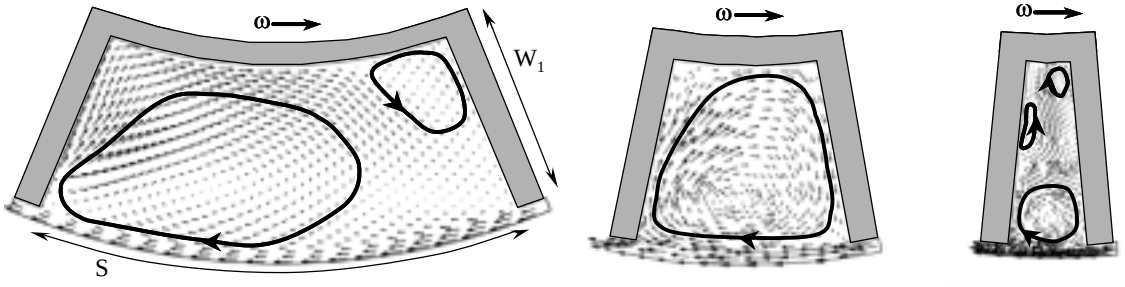

(a) N_B=8 (b) N_B=16 (c) N_B=32

Figure 6 Calculated fluid velocity distributions in r-θ plane at z=20mm

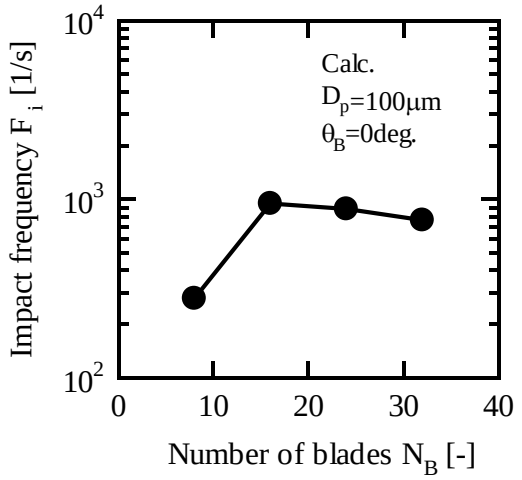

Figure 7 Relationship between impact frequency and number of blades

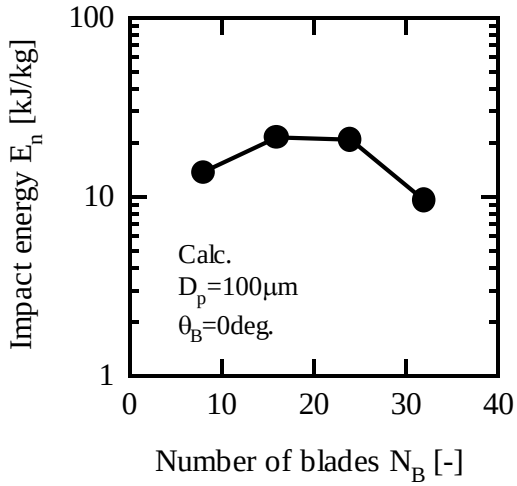

Figure 8 Relationship between impact energy and number of blades

The calculated impact frequency, F_i, which means the total number of impacts with blades and stator per second, is shown in Figure 7. Figure 8 shows the impact energy, E_n, as a function of number of blades. For N_B = 16, particles collide more frequently with the blades and stator wall because of the large swirling flow between blades, as shown in Figure 6 (b). As a result, the impact energy has a maximum value at N_B = 16. The trend for size reduction, as shown in Figure 4, is similar to that for the impact energy, as shown in Figure 8. It can be seen that the grinding performance was improved because the impact energy of particles with blades and stator has a maximum value at N_B = 16.

4.2 Effect of blade angle

4.2.1 Experimental results

Figure 9 shows the median diameter, D_{p50}, of wheat bran powder ground under the rotational speed ω = 14,000min^{-1} and number of blades N_B = 16 as a function of blade angle. The median

diameter decreases with increasing blade angle up to 30° and then increases.

4.2.2 Comparison with calculated results

Figure 10 shows typical particle trajectories for a single particle with a diameter of 100 μm in the mechanical impact mill using various blade angles. The positions of impact on the stator wall are also shown in Figure 10. For the blade angle θ_B = 0°, the particle collides with the blades and the stator wall while moving upward through the mill.

When particles collide with the inclined blades, they are accelerated downwards and move towards the inlet boundary against the airflow. If the particles reached the inlet boundary, they were injected again at the same positions and with a velocity of 0 m/s until they pass through the rotor. It can be seen that the angle of incline of the blade clearly influences the residence time of the particles. In addition, it should be noted that the blade angle has an influence on the number of impacts with the stator wall after the rebound of the particles with the blades, as shown in Figure 10.

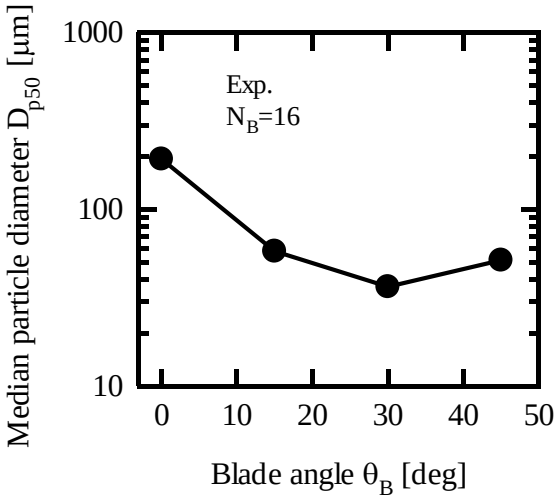

Figure 9 Relationship between median particle diameter and blade angle

For a blade angle of 15°, the particle collides with the stator wall several times after the rebound of the particles from the leading edge of the blades, because a blade inclined at a lower angle leads to a lower rebound velocity in the z-direction. As a result, the particle collides more frequently with the stator wall. On the other hand, for a blade angle of 30°, the particle collides a few times with the stator wall while moving downwards after the rebound from the

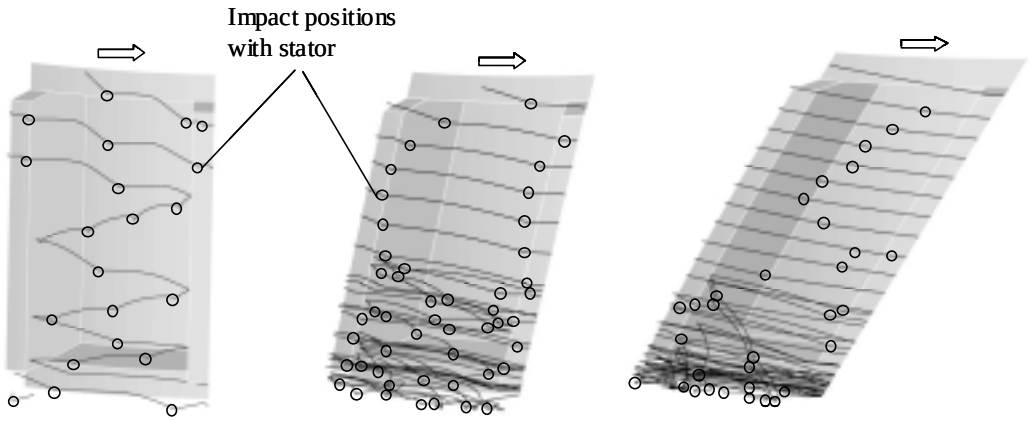

(a) θ_B=0° (b) θ_B=15° (c) θ_B=30°

Figure 10 Typical particle trajectories of a particle with diameter of 100 μm for various blade angles

leading edge of the blade walls because of its higher rebound velocity in the z-direction.

Figure 11 shows the mean residence time of the particles with a diameter of 100 μm as a function of blade angle. As can be seen from Figure 11, the mean residence time increases rapidly with an increase in blade angles from 0 to 15°, and then gradually increases. This is due to the fact that the inclined blades prevent the particles from passing through the rotor directly because the particles are accelerated downwards against the airflow after colliding with the blades.

Figure 12 shows the normal component of impact velocity of particles, v_n, with a diameter of 100 μm as a function of blade angle. The impact velocity decreases with increasing blade angle.

Figure 13 shows the calculated results of the impact energy E_n. It can be seen that the impact energy reaches a maximum value at a blade angle of 30°. The reason for this is due to the balance between the effect of impact velocity and that of residence time. The impact energy depends, not only on the impact velocity of the particle, but on the residence time corresponding to the number of impacts as well. As shown in Figure 12, the normal impact velocity decreases with increasing blade angle. On the contrary, the residence time of particles increases with an increase in blade

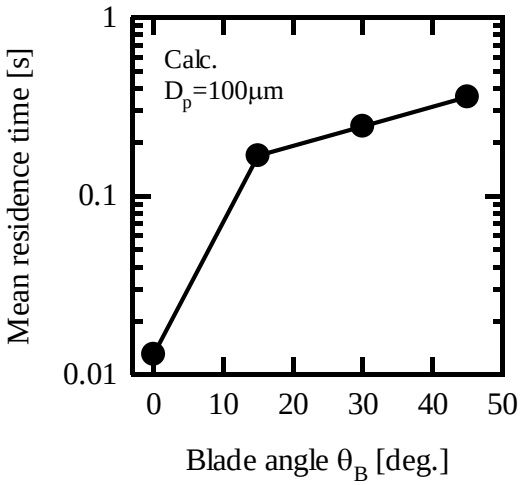

Figure 11 Relationship between mean residence time and blade angle

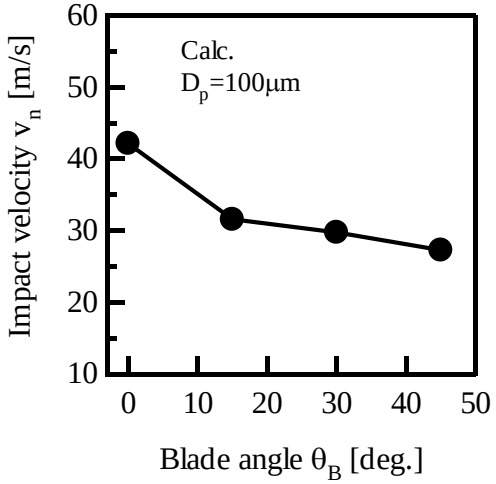

Figure 12 Relationship between impact velocity and blade angle

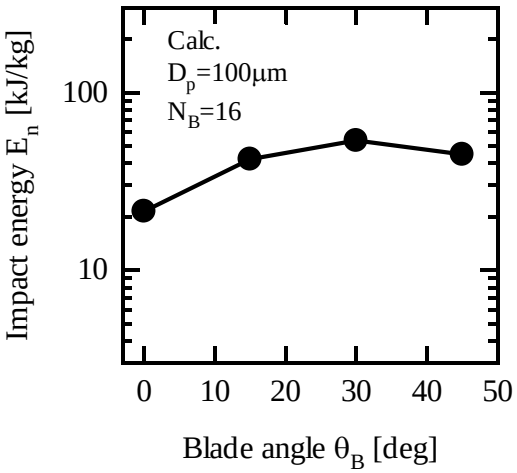

Figure 13 Relationship between impact energy and blade angle

angle, as shown in Figure 11. A blade angle of 30^o results in a longer residence time of particles than that of 15^o and a higher impact velocity than that of 45^o. As a result, the impact energy has a maximum value at a blade angle of 30^o.

5. PERFORMANCE OF THE OPTIMIZED MILL

We have developed a mechanical impact mill with the blades optimized using the numerical simulation technique mentioned above. In this section, the performance of the optimized mechanical mill (Blade Mill BM-15, Nisshin Engineering Inc.) is compared with that of a conventional mechanical mill (SRC-25, Nisshin Engineering Inc.) and a jet mill (Current Jet CJ-10, Nisshin Engineering Inc.).

Figure 14 shows particle size distribution curves for the wheat bran powder ground in the optimized mechanical mill and the conventional mechanical mill under the same conditions. The feed material used here has a mass median diameter of about 500 μm. The median particle diameters for the optimized mechanical mill and the conventional mechanical mill are 9.6 and 35.2 μm, respectively. The maximum particle diameters of powder ground in the optimized mechanical mill and the conventional mechanical mill are 124 and 352 μm, respectively.

Figure 15 shows the relationship between the median particle diameter of product and the specific energy consumption for the optimized mechanical mill, the conventional mechanical mill and the jet mill. The optimized mechanical mill produces powder with a finer and narrower

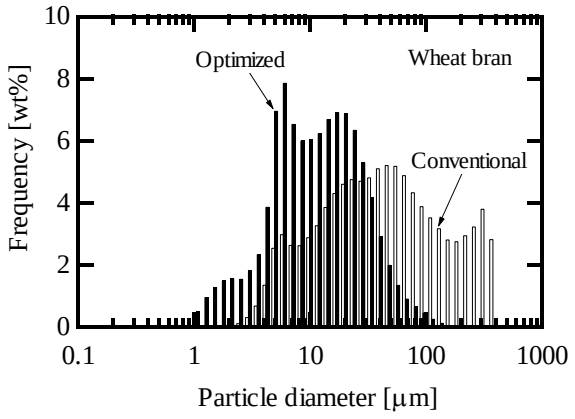

Figure 14 Particle size distributions of wheat bran powder ground in optimized mill and conventional mechanical mill

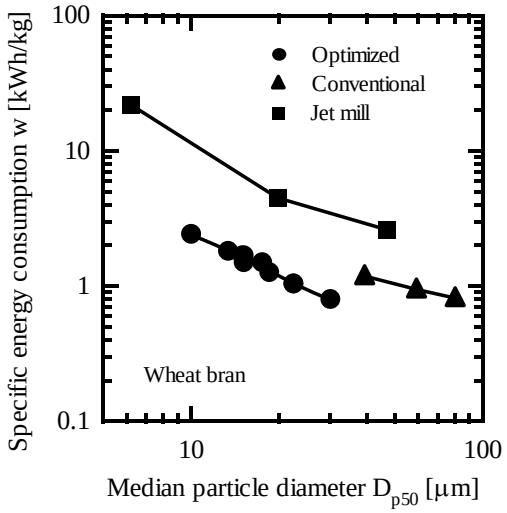

Figure 15 Specific energy consumption as a function of median particle diameter of product for optimized mechanical mill, conventional mechanical mill and jet mill

particle distribution and consumes less energy than the conventional mechanical mill. When powder with a median diameter of 10 μm is produced, the energy consumption for the optimized mechanical mill is 80 % less than that for the jet mill.

6. EFFECT OF GRINDING CONDITIONS ON POWDER PROPERTIES

6.1 Particle size distribution

Particle size distributions of powder ground in the mechanical mill depend on operation conditions including rotational speed, airflow rate and powder feed rate. In particular, the rotational speed is the most important parameter to control them. In order to study the effect of the rotational speed on particle size distributions, dried carrot was ground in the optimized mechanical mill at rotational speeds between 8,000 and 14,000 min^{-1}.

The particle size distributions of dried carrot powder ground at different rotational speeds are shown in Figure 16. The particle size distribution of product shifts to finer sizes as rotational speed increases. The median particle diameters for the rotational speed at 8,000, 12,000 and 14,000 min^{-1} are 18.2, 13.7 and 6.4 μm, respectively. The shapes of the particle size distribution curves are similar although the median particle diameter varies. The maximum particle diameters of carrot powder ground at 8,000, 12,000 and 14,000 min^{-1} are 124.5, 74.0 and 18.5 μm, respectively.

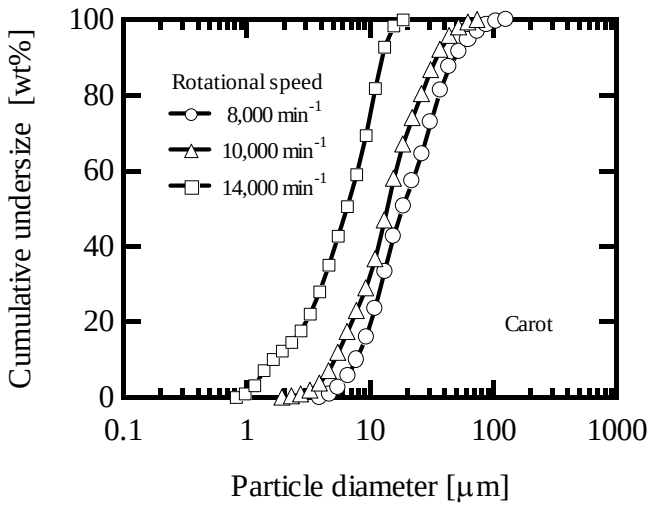

Figure 16 Particle size distributions of dried carrot powder ground in optimized mechanical mill at different rotational speeds

6.2 Color and flavor

Color and flavor of powder are important properties for food materials as well as particle size distributions because they have a great influence on the quality of final products. Effects of grinding temperatures and particle sizes of product on color and flavor of green tea powder have been investigated.

The CIE L^* a^* b^* color coordinates were used to determine the color of green tea powder ground in the optimized mechanical mill under various conditions. The L^* value shows lightness of a color and ranges from black at 0 to white at 100. The a^* value shows red when positive and green when negative, and the b^* value shows yellow when positive and blue when negative. Chroma C^* can be determined from values of the a^* and b^*, which is given by:

$$C^* = \sqrt{(a^*)^2 + (b^*)^2} \qquad (3)$$

Figures 17 and 18 show effect of air temperature at the outlet of the mill on lightness and chroma of the green tea powders with different median diameters. The air temperature in the mill has no significant effect on the lightness and chroma of the green tea powder. However, particle size has a significant effect on the lightness and chroma. As can be seen from Figures 17 and 18, the lightness L^* and chroma C^* increase with decreasing median particle diameter.

Figure 19 shows intensity of flavor for green tea powder ground under various conditions. Flavor intensity was determined using the GC-MS analysis. It can be seen that the flavor intensity decreases with increasing air temperature at the outlet in the mill. In order to prevent from reducing flavor, it is important to control temperature in the mill.

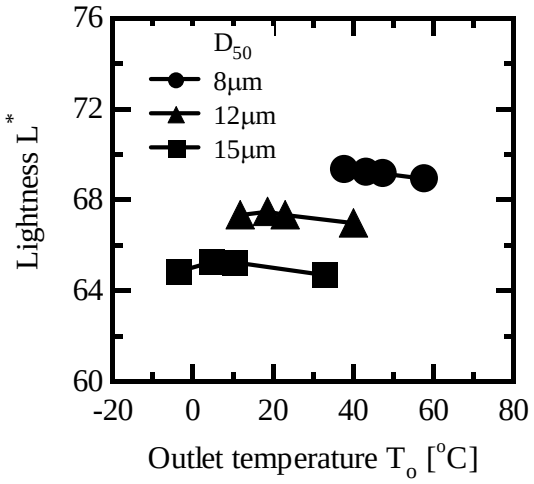

Figure 17 Effect of grinding temperature on lightness of green tea powder for various particle sizes

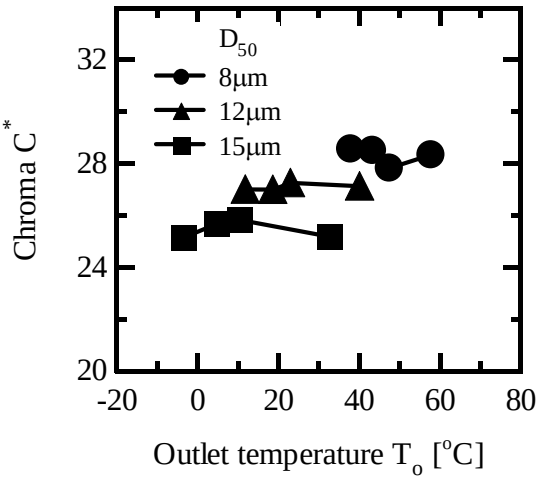

Figure 18 Effect of grinding temperature on chroma of green tea powder for various particle sizes

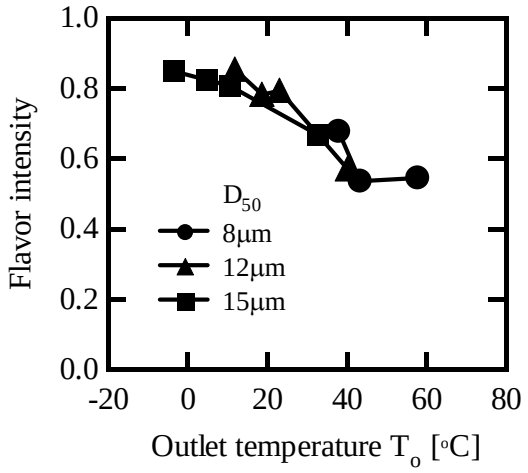

Figure 19 Effect of grinding temperature on flavor of green tea powder for various particle sizes

7. CONCLISIONS

Experimental and numerical studies have been conducted on the effect of blade geometry and operating conditions for a mechanical impact mill. The following conclusions can be made:

(1) The simulated impact energy is one of the most important parameters for determining optimum blade geometry of the mechanical mill.

(2) The mechanical mill with the optimum blade geometry produces powder with a fine and narrow particle distribution compared with the conventional mechanical mill.

(3) Energy consumption of the optimized mechanical mill is 80 % less than that of the jet mill for wheat bran powder with a median diameter of 10 μm.

(4) For green tea powder ground in the mechanical mill, the particle size has a significant effect on the color and the grinding temperature influences the flavor.

NOMENCLATURE

a^*, b^*	=	parameters in the CIE L^* a^* b^* color space	[-]
C^*	=	chroma	[-]
D_p	=	diameter of particles	[μm]
D_{p50}	=	median diameter of particles	[μm]
E_n	=	total impact energy per particle mass	[kJ/kg]
e_n	=	impact energy	[J]
F_i	=	frequency of impact	[1/s]
L^*	=	lightness	[-]
N_B	=	number of blades	[-]
N_a	=	average number of impacts between particles and walls	[-]
N_t	=	total number of injected particles	[-]
n	=	total number of impacts	[-]

r	=	radial coordinate	[mm]
S	=	blade pitch	[mm]
t	=	time	[s]
T_o	=	air temperature at outlet	[^{o}C]
$\boldsymbol{u}$	=	fluid velocity	[m/s]
v_n	=	normal component of particle impact velocity	[m/s]
W_1	=	blade width	[mm]
w	=	power consumption per powder feed rate	[kWh/kg]
z	=	axial coordinate	[mm]

Greek

θ	=	circumferential coordinate	[rad]
θ_B	=	blade angle	[°]
ρ_p	=	particle density	[kg/m^3]
ω	=	rotational speed of rotor blade	[1/min]

REFERENCES

[1] R. Drogemeier and K. Leschonski, *Int. J. Mineral Process*, 44-45 (1996) 485
[2] K. Leschonski and R. Drogemeier, XVIII Int. Mineral Proc.Congress,Sydney (1993) 227
[3] H. Yoshida, T.Saeki, K.Hashimoto and T.Fuyuki, J. of Chem.Eng. of Japan, 24 (1991) 640
[4] S. Akiyama, K. Kozawa and H. Yoshida, WCPT4, Sydney, Australia, No.697 (2002)
[5] T. H. Shih *et al*., *Comp. Fluids*, 24 (1995) 227
[6] S. Akiyama, K. Kozawa and H. Yoshida, *Kagaku Kogaku Ronbunshu*, 30 (2004) 108